CONTRIBUTED
P A P E R

Range Measurement as Practiced in the Deep Space Network

The range of an interplanetary spacecraft can be measured with an accuracy of one meter, even with small signal-to-noise ratios.

By Jeff B. Berner, *Senior Member IEEE*, Scott H. Bryant, and Peter W. Kinman, *Senior Member IEEE*

ABSTRACT | Range measurements are used to improve the trajectory models of spacecraft tracked by the Deep Space Network. The unique challenge of deep-space ranging is that the two-way delay is long, typically many minutes, and the signal-to-noise ratio is small. Accurate measurements are made under these circumstances by means of long correlations that incorporate Doppler rate-aiding. This processing is done with commercial digital signal processors, providing a flexibility in signal design that can accommodate both the traditional sequential ranging signal and pseudonoise range codes. Accurate range determination requires the calibration of the delay within the tracking station. Measurements with a standard deviation of 1 m have been made.

KEYWORDS | Deep Space Network; pseudonoise ranging; range measurement; sequential ranging

I. INTRODUCTION

Range measurement is one of several radiometric techniques used by the Deep Space Network (DSN) to track interplanetary spacecraft [1]. When a spacecraft is in flight, the observables from range measurements are compared with values computed from a model of the trajectory, and discrepancies (called "residuals") are used to improve the model [2].

Within the DSN, the most common type of range measurement is produced by means of two-way coherent ranging. A Deep Space Station (DSS) transmits an uplink carrier whose phase is modulated by a ranging signal. Within the spacecraft transponder, the uplink carrier is demodulated and the recovered ranging signal then phase-modulates the downlink carrier. The DSS receives and demodulates the downlink carrier and measures the round-trip delay of the ranging signal. This technique is coherent because the transponder uses a phase-locked technique to ensure that the uplink and downlink carriers are coherently related.

It is worthwhile considering why the round-trip delay, as opposed to a one-way delay, is measured. If the absolute delay of the downlink signal is measured without having a coherent uplink (or the uplink delay measured without a coherent downlink), the lack of synchronization between the spacecraft and the ground clocks translates directly into an error in the measured delay. The spacecraft clock is the biggest contributor to this error. With a round-trip (two-way) measurement, one clock marks the departure of the ranging signal and its return, and there is no clock synchronization issue.

One-way delay *differences* are measured with excellent accuracy in a technique called differential one-way ranging (DOR) [1]. A DOR measurement employs multiple tones generated in the spacecraft transponder that are phase-modulated onto the downlink carrier. Two DSSs receive the downlink, thus forming an interferometer; and the delay difference is measured. The delay difference is

Manuscript received January 17, 2007; revised April 4, 2007. This work was supported by the National Aeronautics and Space Administration.
J. B. Berner and **S. H. Bryant** are with the Jet Propulsion Laboratory, California Institute of Technology, Pasadena, CA 91109-8099 USA (e-mail: jeff.b.berner@jpl.nasa.gov; scott.h.bryant@jpl.nasa.gov).
P. W. Kinman is with California State University, Fresno, CA 93740 USA (e-mail: pkinman@csufresno.edu).
Digital Object Identifier: 10.1109/JPROC.2007.905128

independent of the spacecraft clock. This technique provides a measure of the angular separation of the spacecraft, within the plane of the interferometer, from a reference direction that is defined by an extragalactic radio source. This technique is used for both spacecraft navigation and for science investigations. Within the DSN, two-way coherent ranging and DOR are considered separate techniques, as they employ different ranging signals and different instrumentation. Moreover, DOR does not provide a measure of the absolute delay. DOR is not discussed further in this paper.

Three-way coherent ranging is similar to two-way coherent ranging. One DSS transmits the uplink carrier and a second DSS receives the downlink carrier. The delay measured in this way is not simply related to range, since the ranging signal does not execute a round trip. Nonetheless, the observables of three-way ranging can be compared with values computed from a trajectory model, providing feedback for the model. Three-way delay data are less accurate than two-way delay data. This is a consequence of clock offsets between the two DSSs as well as an inability to accurately calibrate three-way delay. Three-way ranging is useful when the round-trip delay is large.

The most accurate range measurements are made under the condition that the uplink and downlink carriers are coherently related. Uplinks in the band 2110–2120 MHz (S-band) and also the band 7145–7190 MHz (X-band) are used in the DSN. The spacecraft transponder generates a downlink carrier frequency equal to the uplink carrier frequency multiplied by a rational number, the transponding ratio. The downlink is in the band 2290–2300 MHz (S-band), 8400–8450 MHz (X-band) or 31 800–32 300 MHz (Ka-band). Some transponding ratios are given in Table 1. (Other values have been used as well.)

A command signal will sometimes modulate the phase of the uplink carrier, and a telemetry signal will almost always modulate the phase of the downlink carrier. The command signal does not fully modulate the uplink carrier, and the telemetry signal does not fully modulate the downlink carrier when a ranging signal is present. A residual carrier is therefore present on both the uplink and the downlink during ranging operations. The DSN instrumentation is not designed to extract a range measurement from a suppressed-carrier downlink. Some care must be taken in signal design to ensure that the telemetry and ranging sidebands do not interfere [3].

Table 1 Transponding Ratios

Uplink Band	Downlink Band	Transponding Ratio
S	S	240/221
S	X	880/221
X	X	880/749
X	Ka	3344/749

As part of the Network Simplification Project (NSP), the DSN has new instrumentation for ranging [4]. Previous to this, ranging was done in the DSN using sequential square-wave ranging and a mix of analog and digital signal processing [5], [6]. With the NSP, the processing of the ranging signal is programmed on a commercial processor [7]. Both sequential ranging and pseudonoise (PN) ranging can be supported with a common set of instrumentation. Also, sequential ranging is now done with sine-waves in order to improve spectral efficiency.

This paper is organized as follows. The basis of phase delay measurement is given in Section II. The current NSP instrumentation at the DSN is described in Section III. Calibration of the delay, which is essential for accurate measurement, is discussed in Section IV. The structure of ranging signals, both sequential and pseudonoise, is explained in Section V. The effects of spacecraft receiver noise and DSS receiver noise are analyzed in Section VI.

II. MEASUREMENT DESCRIPTION

This description applies to both two-way and three-way coherent ranging. The abbreviations S_T and S_R represent the transmitting DSS and the receiving DSS, respectively. In the case of two-way coherent ranging, these two stations are the same.

A range measurement consists in sending a ranging signal over a path and measuring the delay. At S_T, a ranging signal is generated and its phase recorded periodically. This ranging signal phase-modulates the uplink carrier. At the spacecraft, the uplink carrier is demodulated. For a spacecraft transponder with a turnaround ranging channel, the baseband ranging signal is filtered and amplified before being phase-modulated onto the downlink carrier. At S_R, the downlink carrier is demodulated and the phase of the ranging signal measured and recorded. From the phase measurements at S_T and S_R, the delay may be inferred.

When ranging with a spacecraft in deep space, the downlink ranging signal-to-noise spectral density ratio is typically small. This necessitates a measurement integration time at S_R of many seconds, even minutes, in order to mitigate receiver noise. During this long integration time, the phase changes. In order to measure the phase for a specific point in time, it is essential that the instrumentation reproduce the rate-of-change of the phase. Following is an explanation of how this is accomplished.

A. Doppler Rate Aiding

The ranging signal is coherently related to the uplink carrier. To be precise, the highest frequency component of the ranging signal, called the range clock, has a frequency

equal to the uplink carrier frequency multiplied by a rational number. Denoting the uplink carrier frequency at S_T by f_T, the range clock frequency at S_T equals βf_T, where

$$\beta = 2^{-7-C}, \quad \text{S-band uplink} \tag{1}$$

$$\beta = \frac{221}{749} \cdot 2^{-7-C}, \quad \text{X-band uplink} \tag{2}$$

and where C is an integer called the component number of the range clock. Due to bandwidth limitations in the DSN instrumentation, $C \geq 4$, corresponding to a maximum frequency of approximately 1 MHz for the range clock. Because better measurement accuracy is obtained for a larger range clock frequency, a C of four is used for most range measurements. This corresponds to a range clock frequency of approximately 1 MHz, whether the uplink is in the S- or the X-band. The uplink carrier frequency f_T is often intentionally varied with time during a tracking pass; this is done in order to compensate for a time-varying Doppler effect on the uplink. The range clock frequency changes with f_T.

As received at the spacecraft, the uplink carrier has a frequency that equals $\alpha_U f_T$, where α_U (an implicit function of time) accounts for the Doppler effect on the uplink. The range clock also experiences a Doppler effect and appears at the spacecraft with a frequency equal to $\alpha_U \beta f_T$.

The spacecraft transmits a downlink carrier with a frequency that equals $G\alpha_U f_T$, where G is the transponding ratio. The range clock frequency is unchanged in passing through the transponder; it remains equal to $\alpha_U \beta f_T$.

At S_R, the received carrier frequency equals $\alpha_D G \alpha_U f_T$, where α_D (an implicit function of time) accounts for the Doppler effect on the downlink. Similarly, the received range clock frequency equals $\alpha_D \alpha_U \beta f_T$. On the downlink, the ratio of the range clock frequency to that of the carrier is β/G. Since β and G are both rational numbers, the ratio β/G is as well.

Doppler rate aiding uses accurate measurements of the downlink carrier frequency provided by the carrier-tracking loop in the receiver at S_R. The measured carrier frequency is multiplied by the constant ratio β/G, and this gives an accurate estimate of the received range clock frequency (that is, the rate of change of the range clock phase). From this estimate, a local model of the received ranging signal is constructed, a model that has the same rate of change of phase as the received range clock.

For a spinning spacecraft, the Doppler rate aiding does not provide a completely accurate local model of the range clock phase. A circularly polarized carrier experiences a small frequency shift when entering a spinning (and circularly polarized) antenna. The transponding ratio multiplies the inbound (spacecraft receive) spinning effect, and so the effect is not completely cancelled on the outbound (spacecraft transmit) side. The ranging signal is not multiplied by the transponding ratio and does not experience this small effect. This resulting offset is usually neglected, but it does create a small bias in a metric called the differenced range versus integrated Doppler (DRVID). This metric represents the difference between two different determinations of a range change: that obtained by differencing two range measurements and that obtained by integrating the range-rate as observed through Doppler measurement of the carrier. The DRVID metric is useful for characterizing the dispersive media through which the links pass.

It is possible to make range measurements using a transceiver instead of a coherent transponder at the spacecraft [8]. This is known as noncoherent ranging. In this case, a spacecraft transceiver generates a downlink carrier independently of the uplink carrier. The range clock, while coherent with the uplink carrier, is not coherent with the downlink carrier for this type of measurement. Doppler rate-aiding is done in this case also, but the resulting local model has a rate of change of phase that does not match exactly that of the arriving range clock. A measurement error arises due to slipping of the local model past the arriving range clock during the course of the integration. This error is proportional to the product of the frequency mismatch and the measurement integration time. In practice, the frequency mismatch is reduced by a combination of varying the uplink frequency in order to compensate for the uplink Doppler effect and estimating the frequency of the spacecraft oscillator from which the downlink carrier is derived. This technique can work well when the measurement integration time is small.

B. Phase Measured at S_T and S_R

At S_T, the phase of the range clock is $\psi_T(t)$, a function of time t. It should not be assumed that $\psi_T(t)$ is a linear function of t, corresponding to a constant uplink frequency. In general, the uplink is tuned in anticipation of an uplink Doppler shift in such a way that the uplink carrier arrives at the spacecraft with most of the Doppler shift canceled. This reduces the stress on the carrier tracking loop in the spacecraft transponder. Samples of the phase $\psi_T(t)$ are recorded periodically. From the tuning history of the uplink carrier, the derivative $d\psi_T/dt$ of $\psi_T(t)$ is a known function of time.

At S_R, the phase of the range clock is $\psi_R(t)$. This phase is different from $\psi_T(t)$ because the ranging signal experiences a delay in passing from S_T to S_R by way of the spacecraft

$$\psi_R(t) = \psi_T(t - \tau(t)). \tag{3}$$

Here $\tau(t)$ represents the time delay experienced by the ranging signal arriving at S_R at time t.

The Doppler effect on the ranging signal is accounted for by the time derivative $\dot{\tau}$ of $\tau(t)$. This can be seen by taking the derivative of both sides of (3), substituting $2\pi\alpha_D\alpha_U\beta f_T$ (the angular frequency of received downlink range clock) for $d\psi_R/dt$ and $2\pi\beta f_T$ (the angular frequency of the transmitted uplink range clock) for $d\psi_T/dt$, and solving for $\dot{\tau}$. The result is

$$\dot{\tau} = 1 - \alpha_D\alpha_U. \tag{4}$$

The local model of the ranging signal that is produced at S_R by means of Doppler rate aiding has a phase $\psi_L(t)$ of the form

$$\psi_L(t) = \psi_T(t - \tau(t)) - \varphi. \tag{5}$$

The phase term φ is nearly constant, varying little over the integration time of the range measurement. To the extent that φ is constant, $\psi_L(t)$ has the same rate of change of phase as $\psi_R(t)$. This φ is unknown from the carrier tracking process.

The fact that φ is not perfectly constant is due primarily to the passage of the uplink and downlink through dispersive media, for which the group delay (that is, the phase delay of the range clock) is not proportional to the phase delay of the carrier. The ionosphere and the solar corona are dispersive media. An accurate range measurement requires that φ be approximately constant for the measurement integration time; thus, the dispersive media places an upper limit on the integration time, and this in turn places a lower limit on the ranging signal-to-noise ratio.

The received ranging signal and the local model of the range clock are correlated using a relatively long integration time. The result of the correlation is a determination of φ. At time t_R, the phase $\psi_L(t)$ is sampled and

$$\psi_R(t_R) = \psi_L(t_R) + \varphi. \tag{6}$$

Also

$$\psi_R(t_R) = \psi_T(t_R - \tau(t_R)). \tag{7}$$

The DSN reports the samples $\psi_T(t_T)$ and $\psi_R(t_R)$, as well as their difference, to the mission navigation teams. Also reported is the time history of the uplink tuning, from which $d\psi_T/dt$ is easily determined. The navigation team can determine $\tau(t)$ from these data, as explained in the next section.

$\psi_T(t_T)$ and $\psi_R(t_R)$ are reported in units of phase called range units (RUs) [9]. When the uplink is in the S-band, 1 RU is defined as two cycles of the uplink carrier. When the uplink is in the X-band, 1 RU is defined as two cycles of a hypothetical carrier with frequency equal to 221/749 times the actual uplink carrier frequency. The time delay corresponding to 1 RU depends on the exact frequency of the uplink carrier. For both S-band and X-band uplinks, this is approximately 0.94 ns.

An aspect of the measurement technique described above that is of practical importance is that there are no real-time signals that pass directly between the transmitting and receiving instrumentation. The phase of the uplink ranging signal and that of the downlink ranging signal are recorded, and the ranging data are extracted from the recorded phases. There are two advantages of this implementation. First, it is a modular design that permits great flexibility. Any receiver works with any antenna, allowing the easy substitution of spare units. Secondly, three-way ranging can be done in the same way as two-way ranging, except that two ground stations are employed.

C. Determination of the Delay

The mission navigation team can determine the delay $\tau(t_R)$ from the phase difference $\psi_T(t_T) - \psi_R(t_R)$. First, it is noted that

$$\psi_T(t_T) - \psi_T(t_R - \tau(t_R)) = \int_{t_R - \tau(t_R)}^{t_T} \frac{d\psi_T}{dt}\, dt. \tag{8}$$

Equation (8) is just the fundamental theorem of calculus. Using (7) and (8)

$$\psi_T(t_T) - \psi_R(t_R) = \int_{t_R - \tau(t_R)}^{t_T} \frac{d\psi_T}{dt}\, dt. \tag{9}$$

In (9), all terms but $\tau(t_R)$ are known. The left-hand side of the equation is the difference between the phase at S_T at time t_T and the phase at S_R, known from the correlation, at time t_R. $d\psi_T/dt$ is the known history of the range clock frequency at S_T. The problem is to find the lower limit on the definite integral that makes the integrated history of the frequency equal to the observed phase difference. After a lower limit is found that satisfies (9), the delay $\tau(t_R)$ is easily calculated. This measured delay $\tau(t_R)$ is the time taken by a ranging signal arriving at S_R at time t_R in coming from S_T. The significance of the time t_R is as the time at which $\psi_L(t)$ is sampled and for which $\psi_R(t_R)$ is computed using (6).

There is a lot of flexibility in choosing a time t_T for the sample of the range clock phase at S_T. For the sake of

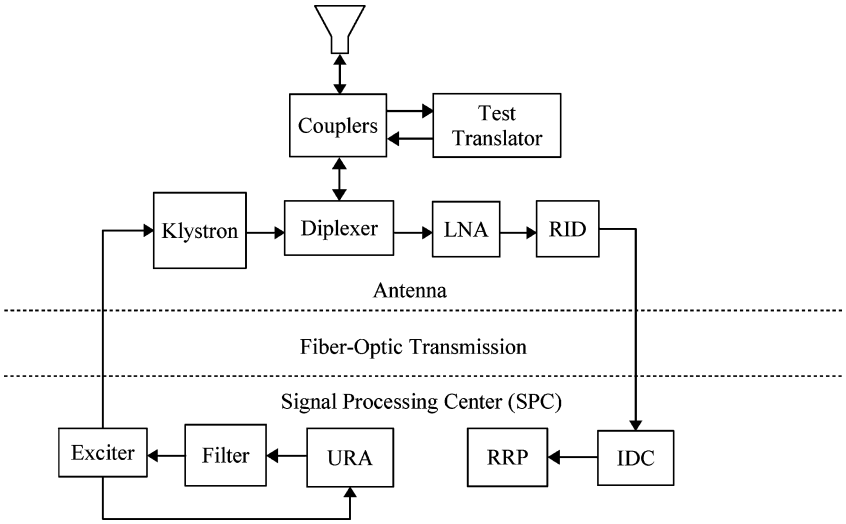

Fig. 1. ***Ranging instrumentation at a deep-space station.***

monitoring the range measurement within the DSN, t_T is chosen equal to t_R, in which case the phase difference of (9) equals simply $2\pi\beta f_T \tau(t_R)$ when the uplink is not tuned. The navigation team, requiring an accurate solution in the general case, will typically select a different value for t_T. For example, a value may be chosen for t_T that is near the difference between t_R and the predicted value of $\tau(t_R)$. In this way, the interval of integration $t_R - \tau(t_R)$ to t_T is minimized.

D. Phase Ambiguity

A subtlety has been overlooked in the above discussion of phase measurement. As is well known, every phase measurement has ambiguity. If the ranging signal consisted only of a range clock, the phases $\psi_T(t_T)$ and $\psi_R(t_R)$ and their difference would only be known modulo 2^{6+C} RU (that is, one cycle of the range clock), where C is the component number of the range clock. In fact, the ranging signal contains more components than just the range clock. The purpose of this additional structure in the signal is to resolve the ambiguity. In general, the phases $\psi_T(t_T)$ and $\psi_R(t_R)$ and their difference have an ambiguity of K RUs, with K an integer larger than 2^{6+C}. The value of K depends on the structure of the ranging signal. Normally, a signal structure is selected for which K is large enough that the actual, absolute delay can be identified from the observed phases with the help of a predicted delay with known tolerances. Section V has more discussion of signal structure and ambiguity resolution.

III. DSS INSTRUMENTATION

Fig. 1 is a schematic diagram of the DSN instrumentation that is used for two-way coherent ranging. The instrumentation is distributed between the antenna and the Signal Processing Center (SPC), which is several kilometers distant from some of the DSS antennas. Microwave and intermediate frequency (IF) signals pass between the antenna and the SPC by means of a fiber-optic transmission system.

The uplink ranging assembly (URA) generates the ranging signal and records its phase; this is done with digital signal processing followed by digital-to-analog conversion. The URA has a two-way connection with the exciter. The exciter provides a frequency reference to the URA, so that the range clock and the uplink carrier are coherently related. The ranging signal passes from the URA through a filter to the exciter, where the ranging signal phase-modulates the uplink carrier. The purpose of the filter is to limit the spectrum. A klystron in the antenna amplifies the carrier before transmission.

The very weak downlink carrier arrives at the antenna and is amplified by a low-noise amplifier (LNA), which can be either a maser or a high electron mobility transistor amplifier. The radio-frequency (RF) signal is downconverted to an IF in the RF-to-IF downconverter (RID). This IF signal is sent to the SPC, where the signal is further downconverted and then digitized in the IF-to-digital converter (IDC). The receiver and ranging processor (RRP) has a phase-locked carrier loop, which provides a coherent reference both for coherent demodulation of the carrier and for Doppler rate aiding. The RRP also incorporates the digital signal processing, on a commercial board, that measures the phase of the received ranging signal. This processing includes the generation of the local model and the correlation of this local model with the received ranging signal.

The description given above applies to three-way coherent ranging also, except that the functions are split between two different DSSs.

IV. CALIBRATION

The dimensions of each DSS antenna are large compared with the desired accuracy of range measurement. Therefore, it is imperative that all delay measurements be referenced to a well-defined point on the DSS antenna. For most DSS antennas, the reference point is the intersection of the azimuth and elevation axes. On the spacecraft also, a reference point is established.

The delay measurement described Section II gives the delay between the URA and the RRP, both located in the SPC. The measured delay must therefore be corrected in order to get the delay from the reference point at S_T to the reference point on the spacecraft and then to the reference point at S_R.

In general, the delay correction will be different from one tracking pass to the next, even for a given DSS. The correction may depend, for example, on the equipment configuration at the DSS and on the band pairing (for example, an S-band uplink paired with an X-band downlink). For this reason, it is essential that the appropriate correction be determined for each tracking pass. To this end, a range calibration is done for each tracking pass that includes ranging.

A range calibration is done immediately before (although sometimes after) a tracking pass. The uplink carrier, modulated by a ranging signal, is intercepted just before being launched by the antenna. This is done with a ranging coupler. A test translator shifts the frequency of the intercepted carrier to a value appropriate for the downlink. This translated carrier is inserted in the downlink path ahead of the LNA. Fig. 1 shows this instrumentation. During the range calibration, the URA and RRP perform the same functions as for two-way coherent ranging, and the resulting delay measurement is called the station delay (STDL). It equals the sum of three partial delays: the delay from the URA to the uplink ranging coupler, the delay through the test translator, and the delay from the downlink ranging coupler to the RRP. The first and third of these partial delays are needed for the correction of an actual two-way coherent range measurement.

The two-way delay from the ranging couplers to the reference point on the DSS antenna must also be characterized. This is an almost constant delay (at a given DSS) that is determined on a relatively infrequent basis using a combination of measurement and calculation.

For two-way coherent ranging, the final, properly referenced, two-way delay is calculated as the measured delay from URA to RRP minus the STDL minus the spacecraft delay plus a term called the Z-correction. The spacecraft delay is measured before the launch of each spacecraft and is a reasonably stable delay. The Z-correction is explained below.

The Z-correction equals the test translator delay minus the two-way delay between the ranging couplers and the DSS antenna reference point. The Z-correction depends on the DSS antenna in question, the location of the ranging couplers, and the band pairing. A table of Z-corrections is maintained for use by the mission navigation teams. This table is updated only infrequently, as the Z-corrections are almost constant.

The correction of the delay for two-way coherent ranging has a typical accuracy of a few nanoseconds [9]. This corresponds to a range accuracy of about 1 m or better.

The correction of three-way coherent ranging data is a special problem. In general, an accurate correction of three-way data is not practical; it would require the separate measurement of the uplink station delay at S_T and the downlink station delay at S_R. In practice, the "corrected" three-way delay is calculated as the measured delay from the URA at S_T to the RRP at S_R minus the average of the (two-way) STDLs at S_T and S_R minus the spacecraft delay plus the average of the (two-way) Z-corrections for S_T and S_R. This procedure gives the right results whenever the delay at S_T is equally divided between uplink and downlink paths and the delay at S_R is equally divided between uplink and downlink paths. Station delay is not, however, actually divided equally between uplink and downlink paths. The three-way ranging phase delays that are sent to the mission navigation teams are, therefore, biased. The amount of this bias has been estimated as about 20 ns.

An additional problem with three-way ranging is the fact that the clocks at S_T and S_R are not synchronized. The time tag t_T for $\psi_T(t_T)$ is based on the clock at S_T and the time tag t_R for $\psi_R(t_R)$ is based on the clock at S_R. The offset between the clocks can be as large as 3 μs. This represents a bias in the three-way time delay. For a given pair of stations, however, this bias is relatively stable. The mission navigation team can usually solve for this bias as part of orbit determination.

V. SIGNAL STRUCTURE

There are two basic types of ranging signal structure in use at the DSN. Sequential ranging signals are described below. Following this are some remarks about PN range codes, including a simple example. References [9] and [10] contain more details on signal structure for sequential and PN ranging, respectively.

For historical reasons, sequential ranging is the standard ranging technique used today in the DSN. However, PN ranging through a turnaround ranging channel offers performance comparable to that of sequential ranging as long as the PN code is chosen with care for the desired performance criteria. The use of a regenerative ranging channel offers a huge improvement in performance over a turnaround ranging channel, and PN ranging is the clear choice when regeneration is to be done in the transponder.

A. Sequential Ranging

At present, the standard signal structure for ranging in the DSN is a sequence of components. This is known as sequential ranging. The first component is the range clock.

Every component has a component number n. The frequency f_n of component n equals a rational number times the carrier frequency. For an S-band uplink

$$f_n = 2^{-7-n} f_T, \quad \text{S-band uplink} \tag{10}$$

and for an X-band uplink

$$f_n = \frac{221}{749} \cdot 2^{-7-n} f_T, \quad \text{X-band uplink} \tag{11}$$

where f_T is the uplink carrier frequency. The first component (the range clock) has component number C, where $C \geq 4$. The component number of the last component is denoted L.

The order of the components in the ranging sequence is: $C, C+1, C+2, \ldots, L$. As indicated by (10) and (11), the frequency of each component (except the range clock) is half that of its predecessor.

The purpose of all components after the first is to resolve the ambiguity in the delay measurement. A range measurement using this technique provides information about the phases $\psi_T(t_T)$ and $\psi_R(t_R)$ (and their difference) modulo K RU, where $K = 2^{6+L}$ RU. The tolerances on the a priori estimate of the delay determine (in an approximate way) K, which in turn dictates L. For example, if the tolerances span 0.03 s, then $K \approx 3.2 \times 10^7$ is adequate (considering that 1 RU corresponds to about 0.94 ns of delay) and the smallest acceptable value for L is then 19.

The range clock is a sine-wave. Some of the succeeding components may be sine-waves as well. Because of the decreasing component frequencies as the sequence progresses, it is not possible for all lower frequency components to appear as sine-waves; this would likely create interference between telemetry and ranging. Instead, the lower frequency components (sometimes all components except the range clock) are subject to chopping.

Each lower frequency component that occurs with chopping takes the form of a square-wave, rather than a sine-wave, and this square-wave multiplies a sine-wave having the frequency of a component, called the "chop component," that occurs earlier in the ranging sequence. Only one chop component is used for a given ranging sequence. Typically, the range clock serves as the chop component. Chopping has the effect of modulating a low-frequency component onto the chop component and the combination onto the carrier, much the same as telemetry data are often modulated onto a subcarrier and the subcarrier onto the carrier. The purpose of this is to shift the spectrum of a low-frequency component to a higher frequency, where it will receive less interference from telemetry. Except to the extent that it prevents interference, chopping has no effect on the performance of sequential ranging. Table 2 shows an example ranging sequence.

At the RRP, an integration time T_1 is used in the correlation of the range clock and an integration time T_2 is used for the correlation of each component following the range clock. T_1 and T_2 are each required to be an integer number of seconds. It is necessary that the RRP be provided with a predicted time delay as well as the start time of the sequence at the transmitting DSS, so that each integration can be started approximately at the arrival time of each new component. When the ranging sequence is generated within the URA, the duration of the range clock is somewhat longer than T_1 in order to accommodate a small error in the predicted delay. The time T for one complete cycle of the ranging sequence is given by [9]

$$T = T_1 + 3 + (L - C)(T_2 + 1) \quad \text{s} \tag{12}$$

Table 2 Example Sequential Ranging Signal

n	f_n (Hz)	waveform	Integration Time
$C = 4$	1,032,000.000	sine-wave (range clock)	$T_1 = 100$ s
5	516,000.000	sine-wave	$T_2 = 2$ s
6	258,000.000	square-wave times range clock	$T_2 = 2$ s
7	129,000.000	square-wave times range clock	$T_2 = 2$ s
8	64,500.000	square-wave times range clock	$T_2 = 2$ s
9	32,250.000	square-wave times range clock	$T_2 = 2$ s
10	16,125.000	square-wave times range clock	$T_2 = 2$ s
11	8,062.500	square-wave times range clock	$T_2 = 2$ s
12	4,031.250	square-wave times range clock	$T_2 = 2$ s
$L = 13$	2,015.625	square-wave times range clock	$T_2 = 2$ s

Table 3 Component PN Codes

n	λ_n	chip sequence (left to right) for one period
1	2	0, 1
2	7	0, 0, 0, 1, 1, 0, 1
3	11	0, 0, 0, 1, 1, 1, 0, 1, 0, 0, 1
4	15	0, 0, 0, 0, 1, 1, 1, 0, 1, 1, 0, 0, 1, 0, 1
5	19	0, 0, 0, 0, 1, 0, 1, 0, 1, 1, 1, 1, 0, 0, 1, 0, 0, 1, 1
6	23	0, 0, 0, 0, 0, 1, 0, 1, 0, 0, 1, 1, 0, 0, 1, 1, 0, 1, 0, 1, 1, 1, 1

where T_1, T_2, and T are each expressed in integer seconds. Following each T_2 slot, there is a 1-s interval during which the signal changes from one component to the next; this accounts for the $T_2 + 1$ appearing in (12). Typically, multiple range measurements are made in a tracking pass; these measurements are spaced T seconds apart.

B. PN Ranging

With PN ranging a composite code is built from component codes, where the component codes have periods that are relatively prime [11]. In this way, the number of chips Λ in one period of the composite code is

$$\Lambda = \prod_{n=1}^{N} \lambda_n \tag{13}$$

where λ_n is the number of chips in one period of component code n and N is the number of component codes. Normally, the first component code is the range clock, with $\lambda_1 = 2$ (representing the positive and negative half-cycles of one period of a sine-wave). For a composite PN code of this type, a range measurement provides information about the phases $\psi_T(t_T)$ and $\psi_R(t_R)$ (and their difference) modulo K RU, where $K = (\Lambda/2) \cdot 2^{6+C}$ RU. (C is the component number of the range clock.) The tolerances on the a priori estimate of the delay determine (in an approximate way) K, which in turn dictates Λ. For example, if the tolerances span 0.5 s, then $K \approx 5 \times 10^8$ is adequate and Λ should be larger than about 1 000 000.

It is desirable to have relatively small periods for the component codes, so that quick acquisition is possible with a reasonable number of parallel correlators [12]. Yet Λ must be large enough to resolve the ambiguity. Equation (13) implies that both goals can be reached with a long composite code built from short codes.

Many codes are possible that are consistent with the above design criteria. One example, borrowed from [10], is given below.

Table 3 specifies a set of six component codes. The periods are the set of relatively prime numbers 2, 7, 11, 15, 19, and 23. The first component corresponds to the range clock. The purpose of components two through six is to resolve the ambiguity.

Each chip of the composite code is determined in the following way. The current chip of each of component codes two through six are input to a logical AND operation. The result of this, which is zero most (31/32) of the time and the current chip of component one (the range clock) are input to a logical OR operation. This gives the current chip of the composite code.

The composite code created in this way has a length Λ of 1 009 470 chips. The ambiguity of this composite code is $K = (1,009,470/2) \cdot 2^{6+C}$ RU. In the typical case $C = 4$, this is 516 848 640 RU or, equivalently, approximately 0.5 s of ambiguity in the time delay.

Pulse shaping is used to reduce the bandwidth of the modulated uplink carrier. Each chip of the composite code having logical value of zero is represented as a positive half-cycle of a sine-wave. Each chip having logical value of one is represented as a negative half-cycle of a sine-wave.

PN codes that are well suited for regenerative ranging are examined in [13] and [14].

C. Comparison of Sequential and PN Ranging

In ranging, power and time may be regarded as the fundamental resources to be husbanded. In addition to minimizing the received power required for a measurement of a given quality, it is also important to minimize the time required for that measurement. This time, denoted T, is the cycle time in sequential ranging and the composite code period in PN ranging. Usually, multiple range measurements are made in a tracking pass. The smaller the T, the more range data can be collected in a tracking pass. With sequential ranging, all the ranging signal power is brought to bear in measuring the phase of the range clock; the price paid is that part of the cycle time must be devoted to the ambiguity-resolving components. With PN ranging, the integration time for the range clock equals the measurement time T; however, not all of the ranging power is available for the range clock. In short, sequential ranging partitions time and PN ranging partitions power.

VI. PERFORMANCE IN NOISE

The performance of the delay measurement in the presence of receiver noise is characterized here. The

following analysis primarily concerns turnaround ranging; however, an approximate result for regenerative ranging is obtained as well.

A. Signal and Noise Analysis

In the following analysis, which incorporates results for both sequential and PN ranging, it is advantageous to use a common model for the ranging signal. The signal model $c(t)\sin\gamma t$ is used here for both types of ranging. In the case of sequential ranging, this model can represent a pure sine-wave by setting $c(t)$ to one and γ to the angular frequency. In the case of sequential ranging with chopping, $c(t) = \pm 1$ represents the square-wave component and $\sin\gamma t$ the chop component. In the case of PN ranging, $c(t)$ is a sequence of binary-valued (± 1) symbols with symbol period equal to π/γ; the product of one symbol of $c(t)$ with one (positive or negative) half-cycle of $\sin\gamma t$ represents one (shaped) chip of the composite PN code. In the analysis that follows, advantage is taken of the fact that in all cases $|c(t)| = 1$.

The uplink carrier as it appears at the spacecraft receiver is of the form

$$\sqrt{2}\sin[2\pi f_U t + \theta c(t)\sin\gamma t]$$

where θ is the peak uplink ranging modulation index in radians, $f_U = \alpha_U f_T$ is the frequency of the arriving uplink carrier, and $\gamma = 2\pi\alpha_U\beta f_T$ is the angular frequency of the arriving range clock. In this model the uplink carrier has unity power. Therefore, in order to get the correct signal-to-noise ratio in this analysis, the one-sided noise spectral density in the spacecraft receiver is taken to be the reciprocal of $P_T/N_0|_U$, where $P_T/N_0|_U$ is the ratio of the total uplink power to the one-sided noise spectral density of the spacecraft receiver.

The fundamental harmonic of the ranging signal is [15]

$$2\sqrt{2}J_1(\theta)c(t)\sin(\gamma t)\cos(2\pi f_U t)$$

where $J_1(\cdot)$ is the Bessel function of the first kind of order one. Also present are other signal elements, such as the residual carrier and higher order harmonics of the ranging signal, but these can be ignored for the present purposes. The residual carrier is in phase-quadrature to the fundamental harmonic of the ranging signal and therefore does not appear in the ranging channel. The higher order harmonics of the ranging signal carry less power than the fundamental and are more greatly attenuated by the ranging channel filter. It is a good approximation, therefore, to consider only the fundamental.

In the transponder, the fundamental is multiplied by a coherent carrier reference (provided by the carrier tracking loop) of the form $\sqrt{2}\cos(2\pi f_U t)$. The result is the baseband signal

$$2J_1(\theta)c(t)\sin(\gamma t)$$

which has a power $2J_1^2(\theta)$. The signal-to-noise ratio ρ in a turnaround ranging channel is

$$\rho = \frac{2J_1^2(\theta)}{B}\cdot\frac{P_T}{N_0}\bigg|_U \tag{14}$$

where B is the noise-equivalent bandwidth of the ranging channel, typically about 1.5 MHz.

An automatic gain control (AGC) circuit in the turnaround ranging channel amplifies the baseband ranging signal and noise before they are sent to the phase modulator for the downlink carrier. The phase deviation $\psi(t)$ of the downlink carrier is of the form

$$\psi(t) = \sqrt{2}\phi_R c(t)\sin(\gamma t) + \phi_N u(t) \tag{15}$$

where ϕ_R and ϕ_N are effective root mean square (rms) modulation indexes (rad) for the ranging signal and the noise, respectively, and $u(t)$ represents zero-mean unity-variance Gaussian noise. The signal-to-noise ratio of $\psi(t)$ is given by

$$\left(\frac{\phi_R}{\phi_N}\right)^2 = \rho. \tag{16}$$

The AGC acts to enforce a constant power in $\psi(t)$

$$\phi_R^2 + \phi_N^2 = \phi_D^2 \tag{17}$$

where ϕ_D is the design value of the rms modulation index (rad) for the downlink ranging channel. Equation (16) and (17) together imply that

$$\phi_R = \phi_D\sqrt{\frac{\rho}{1+\rho}} \tag{18}$$

and

$$\phi_N = \frac{\phi_D}{\sqrt{1+\rho}}. \tag{19}$$

The effective modulation indexes ϕ_R and ϕ_N depend on ρ, whereas ϕ_D is a design constant.

The presence of noise modulation on the downlink carrier has, in principle, two deleterious effects. The first is that a limited resource, downlink power, is wasted (in the form of noise sidebands and intermodulation products involving noise). This can be seen in (18). When $\rho < 1$, as it typically is during deep-space ranging through a turnaround channel, the effective modulation index ϕ_R is less than ϕ_D, typically *much* less than ϕ_D. (For example, when $\rho \leq -20$ dB, which is typical in deep space, $\phi_R \leq 0.1\phi_D$.) The second effect is that the noise sidebands increase the effective noise floor in the downlink receiver. During early mission phase, when uplink and downlink signals are very strong, this second effect can be important [15]. In the typical deep-space scenario, however, only the first effect is important. The present analysis considers only the first effect.

The downlink carrier as it appears at the DSS is of the form

$$\sqrt{2}\sin[2\pi f_D t + \psi(t) + \phi_T d(t)]$$

where ϕ_T is the telemetry modulation index, $f_D = \alpha_D G \alpha_U f_T$ is the frequency of the arriving downlink carrier, and $d(t)$ is the telemetry signal. Deep-space telemetry signals are typically binary valued, $d(t) = \pm 1$, and that is assumed here. The signal model given above has unity power; the receiver noise that accompanies this signal must therefore be regarded as having a one-sided power spectral density equal to the reciprocal of $P_T/N_0|_D$, the ratio of the total downlink power to the one-sided noise spectral density of the downlink receiver.

Within the RRP, the downlink carrier is multiplied by a coherent carrier reference $\sqrt{2}\cos(2\pi f_D t)$. The baseband ranging signal within the RRP is [15]

$$2J_1(\sqrt{2}\phi_R)\cos(\phi_T)e^{-\phi_N^2/2}c(t)\sin(\gamma t).$$

Based on the above, the ratio of the downlink ranging signal power to the one-sided noise spectral density of the downlink receiver is

$$\left.\frac{P_R}{N_0}\right|_D = 2J_1^2(\sqrt{2}\phi_R)e^{-\phi_N^2}\cos^2(\phi_T)\cdot\left.\frac{P_T}{N_0}\right|_D. \tag{20}$$

$P_R/N_0|_D$ is an important figure of merit and depends on both $P_T/N_0|_U$ and $P_T/N_0|_D$. The dependence on the former is through the effective modulation indexes ϕ_R and ϕ_N, as seen in (14), (18), and (19). The dependence on the latter is explicit in (20).

In a typical deep-space turnaround ranging scenario, the signal-to-noise ratio in the ranging channel is very small, $\rho \ll 1$, and the following approximate expression holds:

$$\left.\frac{P_R}{N_0}\right|_D = \rho\phi_D^2 e^{-\phi_D^2}\cos^2(\phi_T)\cdot\left.\frac{P_T}{N_0}\right|_D. \tag{21}$$

Regenerative ranging offers a huge improvement in performance over turnaround ranging. This improvement is available when the transponder employs a tracking circuit that regenerates a nearly noiseless replica of the ranging signal [16]–[18]. The analysis leading up to (20) can be made applicable to regenerative ranging by taking $\phi_N = 0$ and $\phi_R = \phi_D$. This represents the assumption that range measurement performance is limited by the downlink. The result is

$$\left.\frac{P_R}{N_0}\right|_D = 2J_1^2(\sqrt{2}\phi_D)\cos^2(\phi_T)\cdot\left.\frac{P_T}{N_0}\right|_D. \tag{22}$$

When ϕ_D is small ($\phi_D \ll 1$ rad), regenerative ranging achieves a $P_R/N_0|_D$ that is larger than that for turnaround ranging (with the same set of link parameters) by a factor of approximately $1/\rho$, where ρ is the signal-to-noise ratio in the turnaround channel. For example, regenerative ranging has 20 dB more $P_R/N_0|_D$ than turnaround ranging with $\rho = -20$ dB when ϕ_D is small.

$P_R/N_0|_D$ is related to the basic link parameters through $P_T/N_0|_U$ and $P_T/N_0|_D$. Each of the total signal-to-noise spectral density ratios P_T/N_0 can be calculated from an equation of the type

$$\frac{P_T}{N_0} = \frac{PG_TG_R}{kT_{\text{noise}}}\cdot\left(\frac{c}{4\pi R f_C}\right)^2 \tag{23}$$

where P is transmit power, G_T is transmit antenna gain, G_R is receive antenna gain, T_{noise} is receiving system noise temperature, R is range, f_C is carrier frequency, k is Boltzmann's constant, and c is the speed of electromagnetic waves in vacuum.

B. Delay Measurement Accuracy

Receiver noise in the transponder and at the DSN introduce an error into the time delay measurement. For sequential ranging, the standard deviation σ_τ of this error is given by [15], [19]

$$\sigma_\tau = \frac{1}{2\pi f_R\sqrt{2T_1\cdot\left.\frac{P_R}{N_0}\right|_D}} \tag{24}$$

where f_R is the frequency of the range clock. A similar result holds for PN ranging; the differences are that the integration time for the range clock equals the period T of the composite PN code and that the effective $P_R/N_0|_D$ is reduced through multiplication by the square of the cross-correlation factor of the range clock and composite code [19].

In the case of two-way coherent ranging, the range may be determined from the measured two-way delay. The standard deviation of the measured range is $c\sigma_\tau/2$, where c is the speed of electromagnetic waves in vacuum. For example, with a 1-MHz range clock, a standard deviation σ_τ of 6 ns is obtained when the product $T_1 \cdot P_R/N_0|_D$ is 350 (for example, with $P_R/N_0|_D = 3$ dB-Hz and $T_1 = 175$ s). This corresponds to a standard deviation of measured range equal to about 1 m. In general, there is also a bias in the measured delay and the measured range due to imperfect calibration.

C. Probability of Acquisition

An important figure of merit is the probability of acquisition P_{acq}. It is the probability that the ambiguity in the phase delay is correctly resolved. For both sequential and PN ranging, this probability is a function of $P_R/N_0|_D$.

For sequential ranging, P_{acq} is given by [15]

$$P_{\text{acq}} = \left[\frac{1}{2} + \frac{1}{2}\text{erf}\left(\sqrt{T_2 \cdot \frac{P_R}{N_0}\Big|_D}\right)\right]^{L-C} \tag{25}$$

where T_2 is the integration time for each ambiguity-resolving component in the sequence, C is the component number of the range clock, L is the number of the last component, and

$$\text{erf}(x) = \frac{2}{\sqrt{\pi}}\int_0^x e^{-t^2}dt. \tag{26}$$

The calculation of P_{acq} for PN ranging is rather involved. It is described in [19].

D. Ranging Performance Issues

Performance with turnaround ranging is illustrated in Fig. 2. Different combinations of $P_T/N_0|_U$ and $P_T/N_0|_D$ permit range measurements of the same quality. In the case of this figure, the standard deviation of delay error $\sigma_\tau = 2$ ns and the probability of acquisition $P_{\text{acq}} = 95\%$. The range measurement time T, which is the cycle time for sequential ranging and the composite code period for PN ranging, is 200 s for the two upper curves and 500 s for the two lower curves. The following parameters

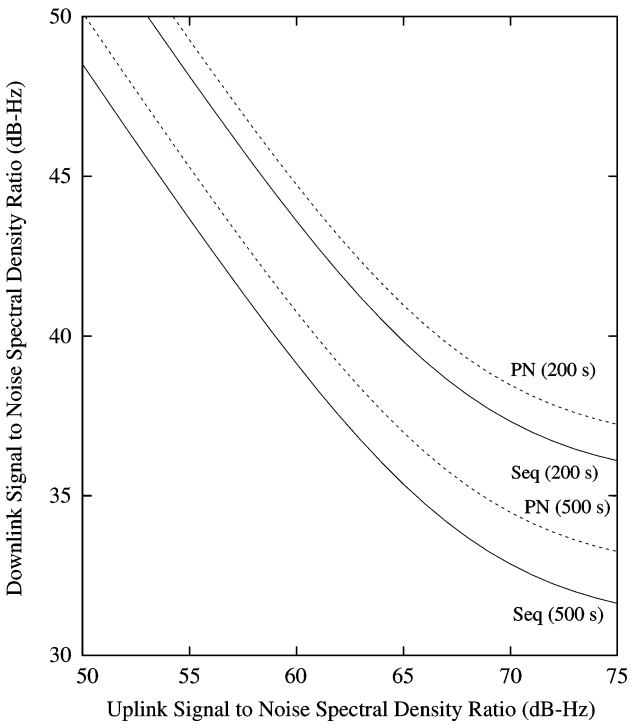

Fig. 2. ***Required levels for 2 ns accuracy with 95% acquisition.***

apply to this figure: $\theta = 0.80$ rad peak, $\phi_D = 0.2$ rad rms, $\phi_T = 1.2$ rad, $f_R = 1.032$ MHz, and $B = 1.5$ MHz. The two curves for PN ranging are based on the example composite PN code discussed in this paper. The two curves for sequential ranging are based on $C = 4$ and $L = 23$ and an optimal selection of T_1 and T_2 such that the cycle time T given by (12) equals 200 or 500 s. With these parameters, sequential ranging can resolve a delay ambiguity of approximately 0.5 s, the same as that for the composite PN code of this example.

In the typical deep-space scenario, $P_T/N_0|_U$ is larger than $P_R/N_0|_D$. This is reflected in the range of values depicted in Fig. 2. This asymmetry results because the transmitter power for the uplink is much larger than that for the downlink and the same pair of antennas are typically used for both links. An exceptional case occurs when the spacecraft employs two antennas: a high-gain transmit-only antenna and a relatively low-gain receive antenna.

The operating point for typical deep-space turnaround ranging lies somewhere on the left-hand side of Fig. 2. In this regime, a 1 dB increase in $P_T/N_0|_U$ permits a 1 dB decrease in $P_T/N_0|_D$. Equation (21) shows this dependence: the figure of merit $P_R/N_0|_D$ is a function of the product $\rho \cdot P_T/N_0|_D$. On the right-hand side of Fig. 2, ϕ_R approaches its asymptotic value ϕ_D and additional increases in $P_T/N_0|_U$ result in diminishing returns.

Fig. 2 shows that a larger measurement time T permits a better tradeoff. This can also be seen in the equations: in

every performance equation, $P_R/N_0|_D$ is multiplied by an integration time (T, T_1, or T_2).

Fig. 2 indicates that for turnaround ranging, a sequential signal design performs slightly better than the example PN composite code for 2-ns accuracy with 95% acquisition. With other performance criteria, PN ranging (with a well chosen PN code) often performs better than sequential ranging. The best choice for the code in PN ranging depends on the performance criteria. Reference [19] offers guidance on the relative performance of sequential and PN ranging.

For regenerative ranging, the operating point lies on the right-hand side of Fig. 2, since the effective modulation index ϕ_R assumes its asymptotic value ϕ_D. This can mean 20 dB or more of improvement in the ranging link budget, relative to turnaround ranging.

Regenerative ranging is best done with a PN range code. In sequential ranging, the transitions from one component to the next would be a logistical difficulty for regenerative ranging.

Despite the performance advantage of regenerative ranging, there are two practical advantages to turnaround ranging. First, the ranging channel in the transponder is simpler for turnaround ranging. Secondly, a transponder with a turnaround ranging channel is more flexible; it can be used for sequential ranging and also for PN ranging with a wide selection of PN range codes.

VII. CONCLUSION

The use of sequential and PN ranging signals for range measurement in the DSN is explained in this paper. The best accuracy is achieved with coherency of the uplink and downlink carriers (and the range clock) and with Doppler rate aiding. This makes large integration times possible, mitigating the noise of the spacecraft and DSN receivers. Calibration is also essential, given the distributed nature of the transmitting and receiving instrumentation at the DSN. Range measurements with a standard deviation of 1 m have been made. There is also a bias due to imperfect calibration. ■

Acknowledgment

The authors would like to acknowledge those who contributed to the design of the NSP ranging instrumentation: H. Baugh, V. Chen, D. Flora-Adams, G. Johnson, E. Law, J. Magallon, J. Makihara, T. Moyer, A. O'Dea, J. R. Smith, and R. Tausworthe.

REFERENCES

[1] C. L. Thornton and J. S. Border, *Radiometric Tracking Techniques for Deep-Space Navigation*. Hoboken, NJ: Wiley-Interscience, 2003.

[2] T. D. Moyer, *Formulation for Observed and Computed Values of Deep Space Network Data Types for Navigation*. Hoboken, NJ: Wiley-Interscience, 2003.

[3] P. W. Kinman, M. K. Sue, T. K. Peng, and J. F. Weese, "Mutual interference of ranging and telemetry," Jet Propulsion Laboratory, Pasadena, CA, TMO Prog. Rep. 42-140. [Online]. Available: http://ipnpr.jpl.nasa.gov/

[4] J. B. Berner and S. H. Bryant, "New tracking implementation in the Deep Space Network," presented at the 2nd ESA Workshop Tracking, Telemetry Command Syst. Space Applicat., Oct. 2001.

[5] J. C. Breidenthal and T. A. Komarek, "Radio tracking system," in *Deep Space Telecommunications Systems Engineering*, J. H. Yuen, Ed. New York: Plenum, 1983, ch. 4.

[6] H. W. Baugh, *Sequential Ranging—How It Works*. Pasadena, CA: Jet Propulsion Laboratory, 1993, Pub. 93-18.

[7] S. Bryant, "Using digital signal processor technology to simplify deep space ranging," presented at the 2001 IEEE Aerosp. Conf., Mar. 2001.

[8] M. K. Reynolds, M. J. Reinhart, R. S. Bokulic, and S. H. Bryant, "A two-way noncoherent ranging technique for deep space missions," presented at the 2002 IEEE Aerosp. Conf., Mar. 2002.

[9] "Sequential ranging," in *DSN Telecommunications Link Design Handbook*, Doc. 810-005, Pasadena, CA, Jet Propulsion Laboratory, module 203B. [Online]. Available: http://eis.jpl.nasa.gov/deepspace/dsndocs/810-005/

[10] "Pseudonoise and regenerative ranging," in *DSN Telecommunications Link Design Handbook*, Doc. 810-005, Pasadena, CA, Jet Propulsion Laboratory, module 214. [Online]. Available: http://eis.jpl.nasa.gov/deepspace/dsndocs/810-005/

[11] R. C. Tausworthe, "Tau ranging revisted," Jet Propulsion Laboratory, Pasadena, CA, TDA Prog. Rep. 42-91. [Online]. Available: http://ipnpr.jpl.nasa.gov/

[12] R. C. Tausworthe and J. R. Smith, "A simplified, general-purpose deep-space ranging correlator design," Jet Propulsion Laboratory, Pasadena, CA, TDA Prog. Rep. 42-92. [Online]. Available: http://ipnpr.jpl.nasa.gov/

[13] J. L. Massey, G. Boscagli, and E. Vassallo, "Regenerative pseudo-noise (PN) ranging sequences for deep-space missions," *Int. J. Satellite Commun. Network.*, vol. 25, no. 3, pp. 285–304, May/Jun. 2007.

[14] J. L. Massey, G. Boscagli, and E. Vassallo, "Regenerative pseudo-noise-like (PNL) ranging sequences for deep-space missions," *Int. J. Satellite Commun. Network.*, vol. 25, no. 3, pp. 305–322, May/Jun. 2007.

[15] P. W. Kinman and J. B. Berner, "Two-way ranging during early mission phase," presented at the 2003 IEEE Aerosp. Conf., Mar. 2003.

[16] J. B. Berner, J. M. Layland, P. W. Kinman, and J. R. Smith, "Regenerative pseudo-noise ranging for deep-space applications," Jet Propulsion Laboratory, Pasadena, CA, TMO Prog. Rep. 42-137. [Online]. Available: http://ipnpr.jpl.nasa.gov/

[17] L. Simone, D. Gelfusa, and M. C. Comparini, "On-board regenerative ranging channel: Analysis, design and test results," presented at the 3rd ESA Workshop Tracking, Telemetry Command Syst. Space Applicat., Sep. 2004.

[18] R. J. DeBolt, D. J. Duven, C. B. Haskins, C. C. DeBoy, and T. W. LeFevere, "A regenerative pseudonoise range tracking system for the New Horizons spacecraft," presented at the 61st Annu. Meeting Inst. of Navigation, Jun. 2005.

[19] J. B. Berner and S. H. Bryant, "Operations comparison of deep space ranging types: Sequential tone vs. pseudo-noise," presented at the 2002 IEEE Aerosp. Conf., Mar. 2002.

ABOUT THE AUTHORS

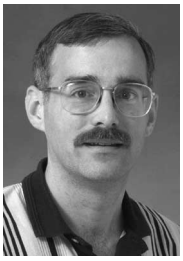

Jeff B. Berner (Senior Member, IEEE) received the B.S. degree (with honors) in electrical engineering and the M.S. degree in electrical engineering from the California Institute of Technology (Caltech), Pasadena, in 1983 and 1984, respectively.

With the exception of a six-month period in 1984, he has been with the Jet Propulsion Laboratory, Caltech, since 1982. Early in his career, he worked on projects such as the Galileo and Mars Observer spacecraft and the Mobile Satellite Experiment (MSAT-X). More recently, he was the Cognizant Development Engineer of the Block V Receiver, the tracking and telemetry receiver of the Deep Space Network. Currently, he is the Development and Operations Chief Engineer for the Deep Space Network.

Mr. Berner received the NASA Exceptional Service Medal in 1996 and the NASA Exceptional Achievement Medal in 2003.

Scott H. Bryant received the bachelor's degree in aeronautics and astronautics engineering from the Massachusetts Institute of Technology, Cambridge.

He is a Member of Senior Staff with the Jet Propulsion Laboratory (JPL), California Institute of Technology, Pasadena. He has worked in the aerospace industry for the last 13 years. He has worked on several of JPL's Deep Space Network (DSN) systems since 1990, including the receivers, exciters, and spacecraft tracking subsystems. He has been principally involved with software design and development for spacecraft tracking, including as Cognizant Design Engineer for the current DSN sequential ranging assembly. He is currently the Implementation and Design Lead for the spacecraft tracking and ranging portion of JPL's Network Simplification Project.

Peter W. Kinman (Senior Member, IEEE) was born in Saint Louis, MO, in 1955. He received the B.S. degrees in electrical engineering and physics from the University of Missouri-Rolla and the Ph.D. degree in electrical engineering from the University of Southern California, Los Angeles.

He was with the Jet Propulsion Laboratory, Pasadena, CA, from 1979 to 1993, where he worked on telemetry and Doppler and range measurements in support of deep-space exploration. From 1993 to 2005, he was a Researcher with Case Western Reserve University, Cleveland, OH. He currently is with California State University, Fresno, specializing in radio technology for space communications.